Low-Resolution Limited Feedback for mmWave NOMA Communications

Yavuz Yapıcı, İsmail Güvenç, and Huaiyu Dai
Department of Electrical and Computer Engineering, North Carolina State University, Raleigh, NC
{yyapici,iguvenc,hdai}@ncsu.edu

***Abstract*—The spectrum-efficient millimeter-wave (mmWave) communications has recently attracted much attention as a viable solution to spectrum crunch problem. In this work, we propose a novel non-orthogonal multiple access (NOMA) framework, which makes use of the directional propagation characteristics of mmWave communications so as to improve the spectral efficiency through non-orthogonal signaling. In particular, we consider one-bit quantized angle information as a limited yet effective feedback scheme describing the channel quality of user equipment (UE) in mmWave bands. The UE pairs for NOMA transmission are then established using not only the one-bit distance feedback as a classical approach, but also the one-bit angle feedback. The numerical results verify that the respective transmission scheme, which is referred to as two-bit NOMA, outperforms the sum-rate performance of angle- or distance-only one-bit NOMA schemes. We also investigate impact of the quantization threshold and size of the user region on the overall sum rate performance, which reveal the practical circumstances making the proposed two-bit NOMA a promising strategy.**

***Index Terms*—Limited feedback, low-resolution, mmWave, multiuser communications, NOMA.**

I. Introduction

The number mobile devices around the world has increased unprecedentedly over the last decade, which is reported to reach some 7.9 billion subscriptions in the first quarter of 2019 corresponding to an annual growth rate of 2% [1]. To accommodate the wireless data demanded by this huge amount of mobile user equipment (UE), new communications bands and multiple access schemes have been considered for next-generation cellular networks in the scope of 5G and beyond. The use of millimeter-wave (mmWave) frequency bands has therefore become a promising solution to the spectrum crunch at the communications spectrum below $6\,\text{GHz}$, which occurs especially when the new communications signals of much wider bandwidth are demanded [2]. In an effort to use the spectrum even more efficiently, non-orthogonal multiple access (NOMA) schemes are envisioned as the key technology for densely packed multiuser environments [3]–[5].

The NOMA strategy has attracted much attention recently both for sub-6 GHz and mmWave frequency bands. As a practical situation, the impact of imperfect successive interference cancellation (SIC) is considered for a cooperative cognitive-radio setting in [6], and for a multiple-antenna setting in [7]. The user-pairing problem is considered in [8] for cooperative NOMA transmission. A hybrid NOMA scheme with simultaneous wireless information and power transfer (SWIPT) is proposed in [9], where the harvested energy using the downlink signal is intended to power the system during the uplink phase. NOMA is also considered in unmanned aerial vehicle (UAV) communications under various scenarios including cellular-connected networks and broadband coverage for temporary events [10]–[16], to name a few.

In this study, we propose a novel transmission mechanism for NOMA as a complete framework in mmWave communications. In particular, we exploit the angular sparsity of the mmWave channels, where many of the multipaths show up in a narrow angular window, referred to as angular spread, around the beamforming direction. The angular position of any UE, hence, provides some degree of information on the associated channel quality. Along with the distance between two ends of the transceiver, which describes the channel in a classical way through path loss [11], angle is yet another limited information for mmWave propagation representing the channel quality [12]. The contribution of this work can be summarized as follows:

- We consider both the distance and angle information while forming limited feedback on the UE channel quality required for NOMA transmission. This approach is therefore different from [12] which uses angle information only to construct UE feedback.
- Furthermore, we consider the quantized versions of distance and angle information to cut down the feedback overhead. In particular, we introduce one-bit NOMA, where the single feedback bit represents either the distance or angle, and propose novel two-bit NOMA making use of two feedback bits, where one bit is for the distance, and the other is for angle.
- We also consider particular deployments where the NOMA transmission is not possible (i.e., no UE pair at all), and show how to choose the optimal user to allocate all the spectral resources, referred to as single user transmission (SUT), under such circumstances. The overall sum-rates involving both NOMA and SUT cases are also analytically derived in a rigorous fashion.

To the best of our knowledge, this is the first time in the literature to consider both the one-bit distance and angle information to form feedback on channel quality for NOMA in mmWave frequency bands. The numerical results verify the superiority of the proposed NOMA strategy over not only orthogonal multiple access (OMA) but also the classical one-bit NOMA with the distance-based feedback only.

The rest of the paper is organized as follows. Section II

introduces the system model under consideration. The two-bit NOMA is presented in Section III along with angle- and distance-based one-bit NOMA schemes. The rate derivation is presented in Section IV, and the numerical results verifying the performance superiority of the proposed two-bit NOMA over the one-bit NOMA schemes are provided in Section V. The paper concludes with some final remarks in Section VI.

II. System Model

We consider a multiuser communications scenario in mmWave frequency spectrum, where K UEs with single antenna each served simultaneously by a BS equipped with an M-element uniform linear array (ULA) antenna. The BS employs a stationary precoder $\mathbf{w}$ to transmit UE messages after superposition coding (SC), and the UEs decode their messages following the SIC strategy. The overall transmission mechanism is therefore a type of NOMA for which the UEs are distinguished in the power domain. We assume that all the UEs lie inside a user region which is represented in polar coordinates by the inner-radius d_{min}, the outer-radius d_{max}, and the center angle Δ, as shown in Fig. 1. Note that the user region can be adjusted through the parameters $\{d_{\mathsf{min}}, d_{\mathsf{max}}, \Delta\}$ to describe any communications environment of interest, which is exemplified in [11], [12] considering a UAV-assisted wireless communications scenario intended for temporary events (e.g., stadium events).

We assume that the UEs are represented by the index set $\mathcal{N}_{\mathsf{U}} = \{1, 2, \ldots, K\}$, and are deployed randomly following a homogeneous Poisson point process (HPPP) with density λ. The number of UEs is therefore Poisson distributed with the probability mass function (PMF) $\mathsf{p}_K(k) = \frac{\mu^K e^{-\mu}}{K!}$ where $\mu = (d_{\mathsf{max}}^2 - d_{\mathsf{min}}^2)\frac{\Delta}{2}\lambda$. The channel $\mathbf{h}_k$ for the k-th UE is

$$\mathbf{h}_k = \sqrt{M}\sum_{p=1}^{N}\frac{\alpha_{k,p}}{\sqrt{\mathsf{PL}\,(d_k)}}\,\mathbf{a}(\theta_{k,p}), \tag{1}$$

where N is the number of multipath components, $\mathsf{PL}(d_k)$ is the path loss associated with the horizontal distance d_k between the k-th UE and the BS, $\alpha_{k,p}$ is the complex gain of the p-th multipath which follows standard complex Gaussian distribution with $\mathcal{CN}(0,1)$, and $\theta_{k,p}$ is the angle-of-departure (AoD) of the p-th multipath. Furthermore, the m-th element of the steering vector $\mathbf{a}(\theta_{k,p})$ is given as

$$\Big[\mathbf{a}(\theta_{k,p})\Big]_m = \frac{1}{\sqrt{M}}\exp\left\{-j2\pi\frac{d}{\lambda}\,(m-1)\cos\left(\theta_{k,p}\right)\right\}, \tag{2}$$

for $m = 1, \ldots, M$, where d is the antenna element spacing of ULA, and λ is the wavelength of the carrier frequency.

III. Two-Bit NOMA

In this section, we first described the NOMA strategy with coding and decoding schemes under consideration, and then present the low-resolution limited feedback schemes based on distance and angle information considering mmWave channels.

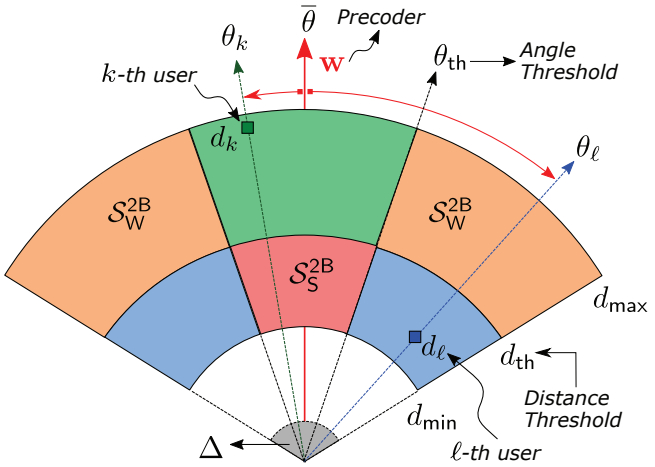

Fig. 1. Polar representation of user region partition for two-bit NOMA in a multiuser mmWave communications scenario.

A. NOMA Transmission and Message Decoding

We assume that the UEs in $\mathcal{N}_{\mathsf{U}}$ are indexed from the best to the worst channel based on the feedback transmitted back to the BS on the UE channel qualities. We further assume that a subset of all the UEs, which is denoted by $\mathcal{N}_{\mathsf{N}}$ involving K_{N} elements, take place in NOMA transmission such that $\mathcal{N}_{\mathsf{N}} \subset \mathcal{N}_{\mathsf{U}}$. Following SC scheme, the desired UE messages was gathered to produce the transmit signal, which is given as

$$\mathbf{x} = \sqrt{\mathsf{P}_{\mathsf{Tx}}}\,\mathbf{w}\sum\nolimits_{k\in\mathcal{N}_{\mathsf{N}}}\beta_k s_k, \tag{3}$$

where P_{Tx} is the total downlink transmit power, s_k is the unit-energy message symbol for the k-th UE, $\mathbf{w} \in \mathbb{C}^{M\times 1}$ is the precoder vector, and β_k is the power allocation coefficient for the k-th UE such that $\sum_{k\in\mathcal{N}_{\mathsf{N}}}\beta_k^2 = 1$. Note that although optimal power allocation policies are beyond the scope of this work, we assume that each UE is allocated a certain amount of power which is *inversely* proportional to its channel quality to yield sufficient decoding performance. This power allocation policy yields $\beta_j \le \beta_i$ for $\forall\, j \le i$ with $i, j \in \mathcal{N}_{\mathsf{N}}$ since the UEs are ordered from the best channel quality to the worst.

The received signal at the k-th UE is given as

$$y_k = \mathbf{h}_k^{\mathrm{H}}\mathbf{x} + v_k = \sqrt{\mathsf{P}_{\mathsf{Tx}}}\mathbf{h}_k^{\mathrm{H}}\mathbf{w}\sum\nolimits_{k\in\mathcal{N}_{\mathsf{N}}}\beta_k s_k + v_k, \tag{4}$$

where v_k is the observation noise following a complex Gaussian process with zero mean and variance σ^2, denoted as $\mathcal{CN}(0,\sigma^2)$, with the transmit signal-to-noise ratio (SNR) $\rho = \mathsf{P}_{\mathsf{Tx}}/\sigma^2$. We further assume that the k-th UE has its own quality-of-service (QoS) based target rate $\overline{\mathsf{R}}_k$, and its message s_k is accurately decoded whenever the respective instantaneous data rate exceeds $\overline{\mathsf{R}}_k$.

Exploiting the fact that the UEs with weak channel quality are allocated more power, each UE first decodes the relatively weaker UEs' messages in a sequential fashion starting from the weakest UE. While a message is being decoded, the interfering messages of all the other UEs (having stronger channel quality) is treated as noise. Adopting SIC strategy, each decoded message is then subtracted from the received signal (prior to the decoding of the next weaker UE's message), and the

desired message of that UE is decoded once all the weaker UEs' messages are decoded and cancelled.

Assuming that all the interfering messages of the UEs weaker than m-th UE are decoded accurately at the k-th UE with $m \geq k$, the respective signal-to-interference-plus-noise ratio (SINR) while decoding the m-th UE message is given as

$$\mathsf{SINR}_{m\to k} = \frac{\mathsf{P}_{\mathsf{Tx}}|\mathbf{h}_k^{\mathrm{H}}\mathbf{w}|^2\beta_m^2}{\sum\limits_{l<m,\, l\in\mathcal{N}_{\mathsf{N}}} \mathsf{P}_{\mathsf{Tx}}|\mathbf{h}_k^{\mathrm{H}}\mathbf{w}|^2\beta_l^2 + \sigma^2}, \tag{5}$$

which also represents the SINR of k-th UE while decoding its own message for $m=k$. Note that (5) yields $\frac{\mathsf{P}_{\mathsf{Tx}}}{\sigma^2}|\mathbf{h}_k^{\mathrm{H}}\mathbf{b}|^2\beta_k^2$ when the k-th UE being the strongest one is decoding its own message since no possible l index of the summation in the denominator satisfies $l<k$. Defining the instantaneous rate associated with the k-th UE while decoding m-th UE message as $\mathsf{R}_{m\to k} = \log_2(1+\mathsf{SINR}_{m\to k})$, the respective outage probability for a given number of UEs $K \geq K_{\mathsf{N}}$ is given as

$$\mathsf{P}_{k|K}^{\mathsf{o,NOMA}} = 1 - \mathsf{Pr}\left(\bigcap_{l\geq k,\, l\in\mathcal{N}_{\mathsf{N}}} \mathsf{R}_{l\to k} > \overline{\mathsf{R}}_l\right), \tag{6}$$

$$= 1 - \mathsf{Pr}\left(\bigcap_{l\geq k,\, l\in\mathcal{N}_{\mathsf{N}}} \mathsf{SINR}_{l\to k} > \epsilon_l\right), \tag{7}$$

where $\epsilon_k = 2^{\overline{R}_k} - 1$. Note that (6) ensures that the k-th UE decodes its message successfully only if it can decode all the messages of the relatively weaker UEs. We therefore ignore *error propagation* due to the unsuccessful decoding of interfering message of any weaker UE, which would be an interesting future topic to investigate. The overall sum rate is

$$\mathsf{R}^{\mathsf{NOMA}} = \sum_{n=K_{\mathsf{N}}}^{\infty} \mathsf{Pr}(K=n)\left(\sum_{k\in\mathcal{N}_{\mathsf{N}}}\left(1-\mathsf{P}_{k|K}^{\mathsf{o,NOMA}}\right)\overline{\mathsf{R}}_k\right). \tag{8}$$

Depending on the NOMA user pairing strategy and the feedback mechanism (on the UE channel qualities), it is not always possible to form a NOMA user group involving K_{N} UEs. We therefore assume a hybrid transmission strategy such that the time-frequency resources and transmit power are fully allocated to a single user whenever NOMA transmission is not possible, and refer to this specific scheme as *single user transmission* (SUT). We consider the problem of choosing the best UE to schedule during SUT in Section III-C, and assume a situation where the mechanism schedules the k_{SUT}-th UE for SUT. The respective outage probability is then given as

$$\mathsf{P}_{k_{\mathsf{SUT}}|K}^{\mathsf{o,SUT}} = \mathsf{Pr}\left(\log_2\left(1+\rho\,|\mathbf{h}_{k_{\mathsf{SUT}}}^{\mathrm{H}}\mathbf{w}|^2\right) \leq \overline{\mathsf{R}}_{\mathsf{SUT}}\right), \tag{9}$$

where $\overline{\mathsf{R}}_{\mathsf{SUT}}$ denotes the QoS-based target rate for any UE when scheduled for SUT. The associated data rate is given as

$$\mathsf{R}^{\mathsf{SUT}} = \sum_{n=1}^{\infty} \mathsf{Pr}(K=n)\left(1-\mathsf{P}_{k_{\mathsf{SUT}}|K}^{\mathsf{o,SUT}}\right)\overline{\mathsf{R}}_{\mathsf{SUT}}. \tag{10}$$

By (8) and (10), the respective hybrid sum rate is given as

$$\mathsf{R}^{\mathsf{HYB}} = \mathsf{P}_{\mathsf{NOMA}}\,\mathsf{R}^{\mathsf{NOMA}} + \mathsf{P}_{\mathsf{SUT}}\,\mathsf{R}^{\mathsf{SUT}}, \tag{11}$$

where $\mathsf{P}_{\mathsf{NOMA}}$ and $\mathsf{P}_{\mathsf{SUT}}$ stand for the probability of occurrence of NOMA and SUT events, respectively.

B. Angle-Based Low-Resolution Feedback

As discussed in the previous section, the power allocation policy dictates that each UE is allocated a certain amount of power which is inversely proportional to its channel quality. The NOMA transmitter therefore requires each UE to feedback an appropriate information describing its channel quality. Considering (5), the term $|\mathbf{h}_k^{\mathrm{H}}\mathbf{w}|^2$ completely describes the channel quality, and, hence, is referred to as *effective channel gain*. Assuming that $\mathbf{w}=\mathbf{a}(\overline{\theta})$ with $\overline{\theta}$ being the AoD of the precoder vector, and incorporating the channel model in (1), the effective channel gain is obtained as

$$|\mathbf{h}_k^{\mathrm{H}}\mathbf{b}|^2 = \sum_{p=1}^{N_{\mathrm{P}}} \frac{|\alpha_{k,p}|^2 M}{\mathsf{PL}(d_k)} \underbrace{\left|\frac{\sin\left(\frac{\pi M(\sin\overline{\theta}-\sin\theta_{k,p})}{2}\right)}{M\sin\left(\frac{\pi(\sin\overline{\theta}-\sin\theta_{k,p})}{2}\right)}\right|^2}_{\mathsf{F}_M(\overline{\theta},\theta_{k,p})}, \tag{12}$$

where $\mathsf{F}_M(\overline{\theta},\theta_{k,p})$ is the Fejér Kernel function [**?**].

Although the effective channel gain in (12) describes the channel quality completely, it becomes computationally complicated to estimate the term $|\mathbf{h}_k^{\mathrm{H}}\mathbf{w}|^2$ as the underlying channel experiences rapid fluctuations over time that requires either frequent estimation from the scratch or sophisticated tracking algorithms [17]. In addition, large number of transmit antennas makes the possible estimation and tracking algorithms computationally even more expensive. Note that the effective channel gain is a function of the distance d_k and the angle $\theta_{k,p}$, both of which vary slowly as compared to the small-scale fading $\alpha_{k,p}$ which is behind the rapid channel fluctuations. The angle and distance information are therefore considered separately in [12] as *limited feedback* for NOMA transmission, which turns out to be powerful alternatives of sending the complete effective channel gain back to the transmitter.

In this work, we propose to use the *low-resolution* versions of the distance and angle information not only *individually* (i.e., either the angle or distance) but also *jointly* (i.e., both the angle and distance). In particular, we consider one-bit quantized feedback information, which corresponds to thresholding the distance and angle with the adequate threshold values d_{th} and θ_{th}, respectively. Each UE therefore computes the one-bit feedback information for both the distance and angle, and sends them back to the NOMA transmitter.

The feedback information, which involves two bits for each UE, is then processed at the NOMA transmitter to split the UEs into two groups based on the channel qualities being strong or weak. When the NOMA transmitter employs both the feedback bits, which is referred to as *two-bit NOMA*, the strong and weak UE groups are defined, respectively, as

$$\mathcal{S}_{\mathsf{S}}^{\mathsf{2B}} = \left\{k\in\mathcal{N}_{\mathsf{U}} \,|\, |\overline{\theta}-\theta_k| \leq \theta_{\mathsf{th}}, d_k \leq d_{\mathsf{th}}\right\}, \tag{13}$$

$$\mathcal{S}_{\mathsf{W}}^{\mathsf{2B}} = \left\{k\in\mathcal{N}_{\mathsf{U}} \,|\, |\overline{\theta}-\theta_k| \geq \theta_{\mathsf{th}}, d_k \geq d_{\mathsf{th}}\right\}, \tag{14}$$

which exploits the dependency of the effective channel gain on the distance and angle information, as provided by (12). Similarly, the strong and weak UE groups based on angle information only are described, respectively, as

$$\mathcal{S}_{\mathsf{S}}^{\mathsf{A}} = \left\{k\in\mathcal{N}_{\mathsf{U}} \,|\, |\overline{\theta}-\theta_k| \leq \theta_{\mathsf{th}}\right\}, \tag{15}$$

$$\mathcal{S}_{\mathsf{W}}^{\mathsf{A}} = \left\{k\in\mathcal{N}_{\mathsf{U}} \,|\, |\overline{\theta}-\theta_k| \geq \theta_{\mathsf{th}}\right\}, \tag{16}$$

and those for distance information only are

$$\mathcal{S}_{\mathsf{S}}^{\mathsf{D}} = \{k \in \mathcal{N}_{\mathsf{U}} \,|\, d_k \leq d_{\mathsf{th}}\}\,,\; \mathcal{S}_{\mathsf{W}}^{\mathsf{D}} = \{k \in \mathcal{N}_{\mathsf{U}} \,|\, d_k \geq d_{\mathsf{th}}\}\,. \quad (17)$$

When the NOMA transmitter employs only the angle or distance feedback individually, as in (15)-(16) or (17), the respective strategy is categorized as *one-bit NOMA*. Assuming a practical transmission scheme of two UEs being served simultaneously, the NOMA transmitter pairs UEs using these groups such that the strong (weak) UE is picked up from $\mathcal{S}_{\mathsf{S}}^{\mathsf{t}}$ ($\mathcal{S}_{\mathsf{W}}^{\mathsf{t}}$) arbitrarily with $\mathsf{t} \in \{\mathsf{2B}, \mathsf{A}, \mathsf{D}\}$. By this way, each pair consists of UEs with sufficiently *distinctive* channel qualities, which ensures the promised performance of NOMA.

Note that although the distance-based one-bit NOMA is considered in [**?**], there is neither angle-based one-bit NOMA nor two-bit NOMA strategies available in the literature for conventional radio-frequency (RF) communications. Considering the directional transmission feature of the mmWave communications, the angle information, however, play a crucial role in describing the channel quality of mmWave links. The numerical results of Section V verify the superiority of the use of angle information in both one-bit and two-bit NOMA for mmWave communications. Note also that more than two UEs can also be scheduled simultaneously within this framework, but at the expense of loosing practicality and degraded SIC decoding performance due to worse performance of UE separation in terms of channel qualities.

C. UE Selection Strategies for SUT

We finally consider the UE selection strategies for the SUT scheme, which takes places whenever the transmitter cannot set up a UE pair, and, hence, the NOMA transmission is not feasible. Indeed under any circumstances, the best UE to schedule during SUT is the one with the best channel quality. However, since the channel quality of any UE is not available fully at the transmitter, we therefore need to determine the best UE based on available limited and low-resolution feedback.

Assuming that the compound two-bit feedback information is available at the transmitter, the best UE to schedule can be found by searching the UE groups using the order $\mathcal{S}_{\mathsf{S}}^{\mathsf{2B}} \rightarrow \mathcal{S}_{\mathsf{W}}^{\mathsf{2B}}$. In this mechanism, whenever at least a single UE is present in $\mathcal{S}_{\mathsf{S}}^{\mathsf{2B}}$, the SUT scheme chooses that UE without proceeding to the next group (i.e., $\mathcal{S}_{\mathsf{W}}^{\mathsf{2B}}$). Similarly, when either the angle or distance information is available only, the best UE to schedule for SUT can be found by searching $\mathcal{S}_{\mathsf{S}}^{\mathsf{s}} \rightarrow \mathcal{S}_{\mathsf{W}}^{\mathsf{s}}$ with $\mathsf{s} \in \{\mathsf{A}, \mathsf{D}\}$.

IV. Hybrid Sum Rate Derivation

In this section, we consider derivation of the outage and event probabilities for the NOMA and SUT schemes under two-bit NOMA transmission strategy to compute the hybrid sum rates given by (11). We start with the analytical expression for the cumulative distribution function (CDF) of the effective channel gain, in the following theorem, and present two additional theorems on derivation of the outage and event probabilities separately.

Theorem 1: The CDF of the effective channel gain for two-bit NOMA with $\mathsf{s} \in \{\mathsf{W}, \mathsf{S}\}$ denoting the type of NOMA UE being weak or strong, respectively, is given as

$$\mathsf{F}_{\mathsf{s}}(x) = \frac{1}{\xi_{\mathsf{s}}} \int_{\mathcal{R}_d^{\mathsf{s}}} \int_{\mathcal{R}_\theta^{\mathsf{s}}} \left(1 - \exp\left\{-\frac{1+r^\gamma}{\mathsf{F}_M(\bar{\theta},\theta)} \frac{x}{\sigma^2}\right\}\right) r \,\mathrm{d}r \,\mathrm{d}\theta, \quad (18)$$

where $\xi_{\mathsf{W}} = (\Delta/2 - \theta_{\mathsf{th}})\big(d_{\mathsf{max}}^2 - d_{\mathsf{th}}^2\big)$, $\xi_{\mathsf{S}} = \theta_{\mathsf{th}}\big(d_{\mathsf{th}}^2 - d_{\mathsf{min}}^2\big)$, $\mathcal{R}_d^{\mathsf{W}} = [d_{\mathsf{th}}, d_{\mathsf{max}}]$, $\mathcal{R}_d^{\mathsf{S}} = [d_{\mathsf{min}}, d_{\mathsf{th}}]$, $\mathcal{R}_\theta^{\mathsf{W}} = [\bar{\theta} - \Delta, \bar{\theta} - \theta_{\mathsf{th}}] \cup [\bar{\theta} + \theta_{\mathsf{th}}, \bar{\theta} + \Delta]$, $\mathcal{R}_\theta^{\mathsf{S}} = [\bar{\theta} - \theta_{\mathsf{th}}, \bar{\theta} + \theta_{\mathsf{th}}]$.

Theorem 2: The outage probability for two-bit NOMA is

$$\mathsf{P}_{k|K}^{\mathsf{o,NOMA}} = \mathsf{F}_{\mathsf{s}}\left(\gamma_{\mathsf{s}}/\rho\right), \quad (19)$$

where $\mathsf{s} \in \{\mathsf{W}, \mathsf{S}\}$ denotes weak and strong NOMA UEs, respectively, with the corresponding indices k_{W} and k_{S}, the variable γ_{s} is given as $\gamma_{\mathsf{W}} = \eta_{\mathsf{W}}$ and $\gamma_{\mathsf{S}} = \mathsf{max}\left(\eta_{\mathsf{W}}, \eta_{\mathsf{S}}\right)$ where

$$\eta_{\mathsf{W}} = \left[\frac{\beta_{\mathsf{W}}^2}{2^{\overline{\mathsf{R}}_{k_{\mathsf{W}}}} - 1} - \beta_{\mathsf{S}}^2\right]^{-1}, \quad \eta_{\mathsf{S}} = \left[\frac{\beta_{\mathsf{S}}^2}{2^{\overline{\mathsf{R}}_{k_{\mathsf{S}}}} - 1} - \beta_{\mathsf{W}}^2\right]^{-1}. \quad (20)$$

Similarly, the outage probability for SUT transmission is

$$\mathsf{P}_{k_{\mathsf{SUT}}|K}^{\mathsf{o,SUT}} = \mathsf{F}_{\mathsf{s}}\left(\left(2^{\overline{\mathsf{R}}_{\mathsf{SUT}}} - 1\right)/\rho\right), \quad (21)$$

where $\mathsf{s} = W$ if $k_{\mathsf{SUT}} \in \mathcal{S}_{\mathsf{W}}^{\mathsf{2B}}$, and $\mathsf{s} = S$ if $k_{\mathsf{SUT}} \in \mathcal{S}_{\mathsf{S}}^{\mathsf{2B}}$.

Theorem 3: The probability of occurrence of two-bit NOMA transmission is given as

$$\mathsf{P}_{\mathsf{NOMA}} = \sum_{K=1}^{\infty} \sum_{n=1}^{K} \sum_{m=1}^{K-n} \mathcal{B}_K(n,m) p_{\mathsf{s}}^n p_{\mathsf{w}}^m \times (1 - p_{\mathsf{s}} - p_{\mathsf{w}})^{K-n-m} \,\mathrm{e}^{-\mu} \frac{\mu^K}{K!}, \quad (22)$$

where $\mathcal{B}_K(n,m) = K!/n!m!(K-n-m)!$ is the multinomial coefficient, $p_{\mathsf{s}} = p_\theta p_d$ and $p_{\mathsf{w}} = (1-p_\theta)(1-p_d)$ are the probabilities for an arbitrary user of being in $\mathcal{S}_{\mathsf{S}}^{\mathsf{2B}}$ and $\mathcal{S}_{\mathsf{W}}^{\mathsf{2B}}$, respectively, with $p_\theta = 2\theta_{\mathsf{th}}/\Delta$ and $p_d = (d_{\mathsf{th}}^2 - d_{\mathsf{min}}^2)(d_{\mathsf{max}}^2 - d_{\mathsf{min}}^2)$. Similarly, probability of occurrence of SUT transmission is given as

$$\mathsf{P}^{\mathsf{SUT}} = \sum_{K=1}^{\infty} \sum_{n=1}^{K} \binom{K}{n} (p_{\mathsf{s}}^n + p_{\mathsf{w}}^n)(1 - p_{\mathsf{s}} - p_{\mathsf{w}})^{K-n} \mathrm{e}^{-\mu} \frac{\mu^K}{K!}, \quad (23)$$

Proof: The proofs of Theorem 1-3 are omitted due to the space limitation in this manuscript and the length of the derivations. The complete proofs will be included rigorously in the journal extension of this paper. ■

Note that employing (19) in (8) and (21) in (10), one can obtain the individual sum rates for NOMA and SUT transmission, respectively. Finally, using the event probabilities of NOMA and SUT given by (22) and (23), respectively, and the individual sum rates in (8) and (10), the hybrid sum rates in (11) can be computed readily.

V. Numerical Results

In this section, we present numerical results based on extensive Monte Carlo simulations, to evaluate the performance of the one-bit and two-bit NOMA strategies for mmWave communications. Considering the mmWave propagation characteristics [18], the simulation parameters are listed in Table I,

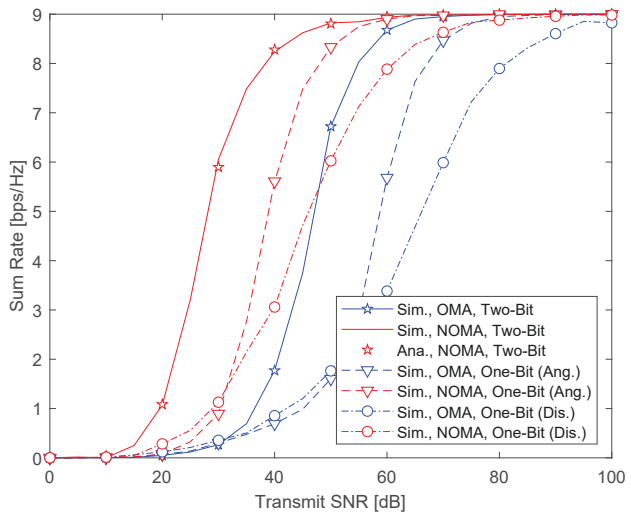

Fig. 2. Hybrid sum-rate performance of one-bit vs two-bit NOMA and OMA along with transmit SNR where $c_\theta = 0.1$ and $c_d = 0.25$.

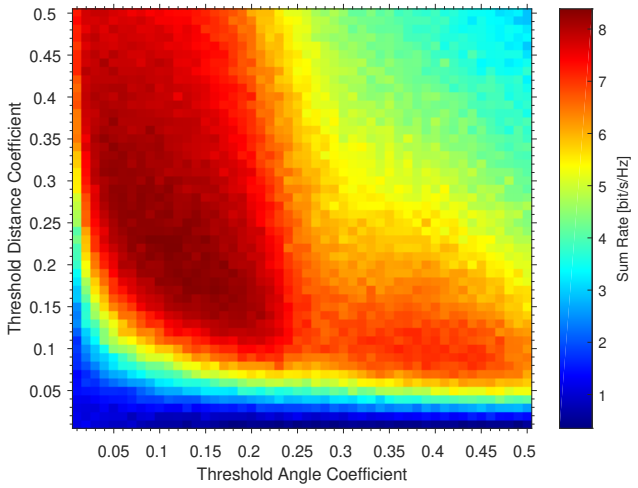

Fig. 3. Hybrid sum-rate performance of two-bit NOMA along with varying angle and distance threshold coefficients with transmit SNR of 30 dB.

where k_{S} and k_{W} denote the indices of strong and weak NOMA UE, respectively. In addition, we assume that the threshold values d_{th} and θ_{th} are obtained using the coefficients $c_d \in [0,1]$ and $c_\theta \in [0,1]$, respectively, through the equations $d_{\mathsf{th}} = d_{\mathsf{min}} + c_d\,(d_{\mathsf{max}} - d_{\mathsf{min}})$ and $\theta_{\mathsf{th}} = c_\theta \Delta/2$.

TABLE I
SIMULATION PARAMETERS

Parameter	Value
UE density (λ)	$0.01\,\mathrm{m}^{-2}$
Number of transmit antennas (M)	64
Path-loss exponent (γ)	2
Power allocation coefficients ($\beta_{k_{\mathsf{W}}}, \beta_{k_{\mathsf{S}}}$)	$(0.6, 0.4)$
Target rate of weak NOMA UE ($\overline{\mathsf{R}}_{k_{\mathsf{W}}}$)	1 bps/Hz
Target rate of strong NOMA UE ($\overline{\mathsf{R}}_{k_{\mathsf{S}}}$)	8 bps/Hz
Target rate of SUT UE ($\overline{\mathsf{R}}_{k_{\mathsf{SUT}}}$)	8 bps/Hz
User region angle (Δ)	15°
User region inner radius (d_{min})	0 m
User region outer radius (d_{max})	30 m
Precoder AoD ($\bar{\theta}$)	0°
Angle threshold coefficient (c_θ)	0.1
Distance threshold coefficient (c_d)	0.25

In Fig. 2, we depict the hybrid sum-rate performance of various NOMA and OMA strategies along with the transmit SNR, where the feedback schemes of one-bit angle only, one-bit distance only, and two-bit (angle and distance together) are considered for both NOMA and OMA transmission. We observe that NOMA is significantly superior to OMA for all the feedback schemes. We also observe that two-bit NOMA employing both the angle and distance feedback bits jointly is much better than one-bit NOMA strategies of distance and angle only, where the theoretical and simulation results show a nice match. Furthermore, one-bit NOMA with angle feedback only yields a better performance than that of distance feedback only. We therefore see that although angle-only one-bit feedback is more powerful than distance-only one-bit feedback in describing UE channel quality for this particular setting, the overall NOMA performance is enhanced even further when both feedback bits are employed (i.e., two-bit NOMA).

We look into the impact of threshold coefficient choice in Fig. 3, which depicts the hybrid sum-rate performance of two-bit NOMA along with varying angle and distance threshold coefficients (i.e., c_θ and c_d, respectively). We observe that while both the coefficients should be taken small enough to have sufficiently stronger UEs in $\mathcal{S}_{\mathsf{S}}^{\mathsf{2B}}$ of (13), the coefficients should not be too small in order not to end up with $\mathcal{S}_{\mathsf{S}}^{\mathsf{2B}}$ having no UE at all. Note that whenever $\mathcal{S}_{\mathsf{S}}^{\mathsf{2B}}$ turns out to be an empty set, the transmission mechanism schedules a single UE (i.e, SUT scheme), and, hence, the hybrid sum-rate performance degrades.

We finally compare the hybrid sum-rate performance of one-bit and two-bit NOMA strategies in Fig. 4 for varying user region size, which is controlled through d_{max} and Δ. In Fig. 4(a), we observe that two-bit NOMA is superior to angle-only one-bit NOMA for $d_{\mathsf{max}} \geq 24\,\mathrm{m}$, for which UEs become more likely to be distinguishable using their distance information, and, hence, two-bit feedback turns out to be more powerful than angle-only one-bit feedback. Note also that as the user region gets smaller (e.g., $d_{\mathsf{max}} \leq 9\,\mathrm{m}$ and $\Delta \leq 3^\circ$), NOMA becomes unfeasible and the transmission scheme switches to SUT, which is the reason for two-bit and angle-only one-bit NOMA having very similar hybrid sum rates.

Similarly, Fig. 4(b) indicates that two-bit NOMA is much better than distance-only one-bit NOMA when the user region is sufficiently large (e.g., $d_{\mathsf{max}} \geq 24\,\mathrm{m}$ and $\Delta \geq 7.5^\circ$). As a result, we conclude that using one more feedback bit representing either distance or angle domain is useful for NOMA transmission only if the UEs are distinguishable in that domain associated with this additional bit of information. In addition, if both distance and angle domain make UEs sufficiently distinctive, two-bit NOMA involving both feedback bits out-

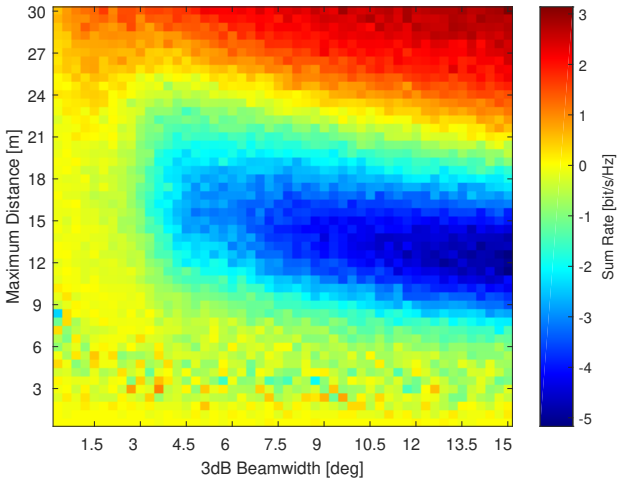

(a) "Two-Bit NOMA" – "Angle NOMA"

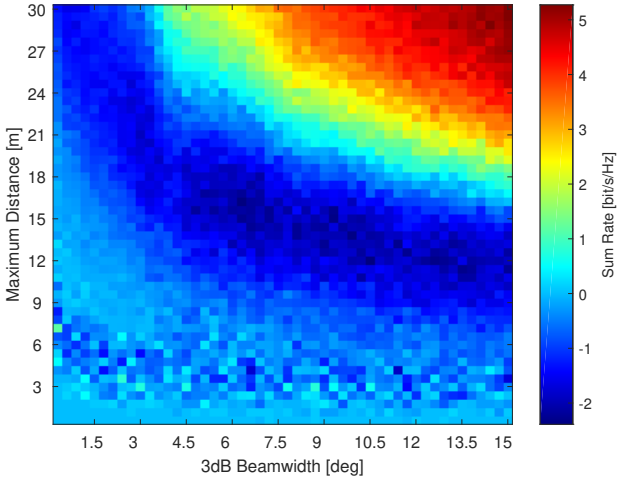

(b) "Two-Bit NOMA" – "Distance NOMA"

Fig. 4. Hybrid sum-rate difference of two-bit and one-bit NOMA for varying $d_{\max}$ and Δ, where $c_\theta = 0.1$ and $c_d = 0.25$, and the transmit SNR is 30 dB.

performs distance- or angle-only one-bit feedback schemes.

VI. Conclusion

We propose a practical NOMA transmission strategy for mmWave communications, which makes use of unique angular propagation characteristics of mmWave links. In particular, we propose a low-resolution feedback mechanism for NOMA, where the distance and angle information of UEs are represented by one bit each. The transmitter groups UEs based on this two-bit information, and sets up UE pairs for NOMA transmission using the groups of UEs having relatively strong and weak channels. The overall transmission mechanism is designed to be hybrid such that all the spectral resources are allocated to a single UE whenever NOMA is not feasible. The numerical results verify the superiority of the proposed one-bit and two-bit NOMA with low-resolution angle information.

References

[1] Ericsson. (2019, Jun.) Ericsson Mobility Report. [Online]. Available: https://www.ericsson.com/en/mobility-report

[2] M. K. Samimi and T. S. Rappaport, "3-D millimeter-wave statistical channel model for 5G wireless system design," *IEEE Trans. Microw. Theory Techn.*, vol. 64, no. 7, pp. 2207–2225, Jul. 2016.

[3] S. M. R. Islam, N. Avazov, O. A. Dobre, and K. Kwak, "Power-domain non-orthogonal multiple access (NOMA) in 5G systems: Potentials and challenges," *IEEE Commun. Surveys Tuts.*, vol. 19, no. 2, pp. 721–742, 2nd Quarter 2017.

[4] Z. Wu, K. Lu, C. Jiang, and X. Shao, "Comprehensive study and comparison on 5G NOMA schemes," *IEEE Access*, vol. 6, pp. 18 511–18 519, Mar. 2018.

[5] L. Dai, B. Wang, Z. Ding, Z. Wang, S. Chen, and L. Hanzo, "A survey of non-orthogonal multiple access for 5G," *IEEE Commun. Tuts.*, vol. 20, no. 3, pp. 2294–2323, 3rd Quarter 2018.

[6] G. Im and J. H. Lee, "Outage probability for cooperative NOMA systems with imperfect SIC in cognitive radio networks," *IEEE Commun. Lett.*, vol. 23, no. 4, pp. 692–695, Apr. 2019.

[7] J. Cui, Z. Ding, and P. Fan, "Outage probability constrained MIMO-NOMA designs under imperfect CSI," *IEEE Trans. Wireless Commun.*, vol. 17, no. 12, pp. 8239–8255, Dec. 2018.

[8] J. Zhang, X. Tao, H. Wu, and X. Zhang, "Performance analysis of user pairing in cooperative NOMA networks," *IEEE Access*, vol. 6, pp. 74 288–74 302, Nov. 2018.

[9] S. K. Zaidi, S. F. Hasan, and X. Gui, "Evaluating the ergodic rate in SWIPT-aided hybrid NOMA," *IEEE Commun. Lett.*, vol. 22, no. 9, pp. 1870–1873, Sep. 2018.

[10] W. Mei and R. Zhang, "Uplink cooperative NOMA for cellular-connected UAV," *IEEE J. Sel. Topics Signal Process.*, vol. 13, no. 3, pp. 644–656, Jun. 2019.

[11] N. Rupasinghe, Y. Yapıcı, I. Güvenç, and Y. Kakishima, "Non-orthogonal multiple access for mmWave drone networks with limited feedback," *IEEE Trans. Commun.*, vol. 67, no. 1, pp. 762–777, Jan. 2019.

[12] N. Rupasinghe, Y. Yapıcı, I. Güvenç, M. Ghosh, and Y. Kakishima, "Angular feedback for mmWave NOMA drone networks," *IEEE J. Sel. Topics Signal Process.*, vol. 13, no. 3, pp. 628–643, Jun. 2019.

[13] T. Hou, Y. Liu, Z. Song, X. Sun, and Y. Chen, "Multiple antenna aided NOMA in UAV networks: A stochastic geometry approach," *IEEE Trans. Commun.*, vol. 67, no. 2, pp. 1031–1044, Feb. 2019.

[14] N. Zhao, X. Pang, Z. Li, Y. Chen, F. Li, Z. Ding, and M. Alouini, "Joint trajectory and precoding optimization for UAV-assisted NOMA networks," *IEEE Trans. Commun.*, vol. 67, no. 5, pp. 3723–3735, May 2019.

[15] T. M. Nguyen, W. Ajib, and C. Assi, "A novel cooperative NOMA for designing UAV-assisted wireless backhaul networks," *IEEE IEEE J. Sel. Areas Commun.*, vol. 36, no. 11, pp. 2497–2507, Nov. 2018.

[16] X. Liu, J. Wang, N. Zhao, Y. Chen, S. Zhang, Z. Ding, and F. R. Yu, "Placement and power allocation for NOMA-UAV networks," *IEEE Wireless Commun. Lett.*, vol. 8, no. 3, pp. 965–968, Jun. 2019.

[17] Y. Yapıcı and I. Güvenç, "Low-complexity adaptive beam and channel tracking for mobile mmWave communications," in *Proc. Asilomar Conf. Signals, Syst., and Comput.*, Pacific Grove, California, Oct. 2018.

[18] T. S. Rappaport, Y. Xing, G. R. MacCartney, A. F. Molisch, E. Mellios, and J. Zhang, "Overview of millimeter wave communications for fifth-generation (5G) wireless networks—with a focus on propagation models," *IEEE Trans. Antennas Propag.*, vol. 65, no. 12, pp. 6213–6230, Dec. 2017.